Energy Conversion and Management 49 (2008) 2656–2668

Contents lists available at ScienceDirect

Energy Conversion and Management

journal homepage: www.elsevier.com/locate/enconman

A robust mixed H_2/H_∞ based LFC of a deregulated power system including SMES

H. Shayeghi [a,*], A. Jalili [b], H.A. Shayanfar [c]

[a] Technical Engineering Department, University of Mohaghegh Ardabili, Ardabil, Iran
[b] Islamic Azad University, Ardabil Branch, Ardabil, Iran
[c] Center of Excellence for Power Automation and Operation, Electrical Engineering Department, Iran University of Science and Technology, Tehran, Iran

ARTICLE INFO

Article history:
Received 4 September 2007
Accepted 13 April 2008
Available online 9 June 2008

Keywords:
LFC
SMES
Restructured power system
Mixed H_2/H_∞ control
Robust control

ABSTRACT

This paper presents a new robust decentralized controller based on mixed H_2/H_∞ control technique for the solution of load frequency control (LFC) problem including superconducting magnetic energy storage (SMES) in a deregulated electricity environment. To achieve decentralization, in each control area, the connections between this area and the rest of the system and the effects of possible contracts are treated as a set of new disturbance signals. In order to minimize effects of load disturbances and to achieve desired level of robust performance in the presence of modeling uncertainties and practical constraints on control action the idea of mixed H_2/H_∞ control technique is being used for the solution of LFC problem. This newly developed design strategy combines advantage of H_2 and H_∞ control syntheses and gives a powerful multi-objectives design addressed by the linear matrix inequalities (LMI) technique. To demonstrate the effectiveness of the proposed method a four-area restructured power system is considered as a test system under different operating conditions. The simulation results with the proposed controller are shown to maintain robust performance in the presence of SMES unit in two areas at power system and without SMES unit in any of the areas. Analysis reveals that the proposed control strategy with considering SMES unit improves significantly the dynamical performances of system such as settling time and overshoot against parametric uncertainties for a wide range of area load demands and disturbances in either of the areas even in the presence of system nonlinearities.

1. Introduction

Global analysis of the power system markets shows that the frequency control is one of the most profitable ancillary services at these systems. This service is related to the short-term balance of energy and frequency of the power systems. The most common methods used to accomplish frequency control are generator governor response (primary frequency regulation) and load frequency control (LFC). The goal of LFC is to reestablish primary frequency regulation capacity, return the frequency to its nominal value and minimize unscheduled tie-line power flows between neighboring control areas. From the mechanisms used to manage the provision this service in ancillary markets, the bilateral contracts or competitive offers stand out [1].

LFC goals, i.e. frequency regulation and tracking the load demands, maintaining the tie-line power interchanges to specified values in the presence of modeling uncertainties, system nonlinearities and area load disturbances determines the LFC synthesis as a multi-objective optimization problem. On the other hand, increasing size and complexity of the restructured power system introduced a set of significant uncertainties and disturbances in power system control and operation, especially on the LFC problem solution. Thus, it is desirable that the novel control strategies be developed to achieve LFC goals and maintain reliability of the electric power system in an adequate level. There have been continuing efforts in design of load frequency controller with better performance according to the change of environment in power system operation under deregulation using various optimal and robust control strategies during the recent years [2–6]. The proposed methods gave good dynamical responses, but robustness in the presence of large modeling uncertainties and system nonlinearities was not considered. Also, in most of the proposed robust methods, only one single norm is used to capture design specifications. It is clear that meeting all LFC design objectives by a single control approach due to increasing the complexity and change of the power system structure is difficult.

In this paper, a new decentralized robust control strategy based on the mixed H_2/H_∞ control technique for solution of the LFC problem in a deregulated power system is proposed. To achieve decentralization, the effects of possible contracted scenarios and connections between each area with the rest of system are treated as a set of new input disturbance signals in each control area. The proposed control strategy combines advantage of H_2 and H_∞ control syntheses to achieve the desired level of robust performance against load disturbances, modeling uncertainties, system

* Corresponding author. Tel.: +98 451 5512910; fax: +98 451 5512904.
E-mail address: hshayeghi@gmail.com (H. Shayeghi).

0196-8904/$ - see front matter © 2008 Elsevier Ltd. All rights reserved.
doi:10.1016/j.enconman.2008.04.006

Nomenclature

F	area frequency
P_{tie}	net tie-line power flow
P_T	turbine power
P_V	governor valve position
P_C	governor set point
ACE	area control error
α	ACE participation factor
Δ	deviation from nominal value
K_P	subsystem equivalent gain
T_P	subsystem equivalent time constant
T_T	turbine time constant
T_H	governor time constant
R	droop characteristic
B	frequency bias
T_{ij}	tie-line synchronizing coefficient between areas i and j
P_d	area load disturbance
P_{Lj-i}	contracted demand of Disco j in area i
P_{ULj-i}	un-contracted demand of Disco j in area i
$P_{m,j-i}$	power generation of GENCO j in area i
P_{Loc}	total local demand
η	area interface
ζ	scheduled power tie-line power flow deviation ($\Delta P_{tie,sch}$)
I_d	inductor current in SMES unit
E_d	converter voltage applied to inductor in SMES unit
K_{SMES}	gain of control loop SMES
K_{id}	the gain for feedback ΔI_d in SMES unit
T_{dc}	converter time constant in SMES unit
u_{SMES}	control signal of SMES unit

nonlinearities and gives a powerful multi-objectives design addressed by the linear matrix inequalities (LMI) techniques [7,8]. Due to its practical merit, it has a decentralized scheme and requires only the area control error (ACE). When a decentralized LFC is applied, by reducing the system size the resulting controller order will be lower, which is ideally useful for the real world complex power systems.

Literature survey shows that, in most of the works concerned with LFC problem [2–6,9,10] of interconnected power systems the supplementary controllers are designed to regulate the area control errors to zero effectively. However, the power frequency and the tie-line power deviations persist for a long duration. In these situations, the governor system may no longer be able to absorb the frequency fluctuations due to its slow response [9]. Thus, to compensate for the sudden load changes, an active power source with fast response such as a superconducting magnetic energy storage (SMES) unit is expected to be the most effective countermeasure. The reported works [11–15] further shows that, SMES is located in each area of the power system for LFC problem. With the use of SMES in all areas, frequency deviations in each area are effectively suppressed. However, it may not be economically feasible to use SMES in every area of a multi-area interconnected power system. Therefore, it is advantageous if an SMES located in an area is available for the control of frequency of other interconnected areas.

Also, literature survey shows that, no work has been carried out for the solution of LFC problem in a deregulated power system considering an SMES unit. In view of the above, SMES units is used to demonstrate technical and economic feasibility of them in deregulated power system applications. The energy storage requirement to damp the frequency oscillations caused by small load perturbations is much smaller. In such cases, the real power transfer takes place in a very short time. Thus, addition of a SMES unit to the system significantly improves transients of frequency and tie-line power deviations against to small load disturbances.

The proposed control strategy is tested on a four-area restructured power system. To damp out the oscillations due to load demands and instantaneous load perturbations as fast as possible, LFC including the mixed H_2/H_∞ controllers is used. Moreover, the considered interconnected power system contains two SMES units in areas 1 and 3, respectively. To illustrate effectiveness of the proposed method two scenarios of possible contracts under different operating conditions are simulated in comparison with the PI controller (which is widely used in practical industries) through some performance indices in the presence of large parametric uncertainties and system nonlinearities under various area load changes. The performance indices are chosen as the integral of the time multiplied absolute value of the error (ITAE) and figure of demerit (FD). The simulation results show that the proposed controller achieves good robust performance for a wide range of system parameters and area load disturbances changes even in the presence of generation rate constraints (GRC). Moreover, analysis of controller resulting show hat with considering SMES unit in same areas dynamical performances of system such as frequency oscillation and settling time significantly is improved due to any large load changes.

2. SMES model

The schematic diagram in Fig. 1 shows the configuration of a thyristor controlled SMES unit. In the SMES unit, a DC magnetic coil is connected to the AC grid through a power conversion system (PCS) which includes an inverter/rectifier. The superconducting coil is contained in a helium vessel. Heat generated is removed by means of a low-temperature refrigerator. Helium is used as the working fluid in the refrigerator as it is the only substance that can exist as either a liquid or a gas at the operating temperature which is near absolute zero. The current in the superconducting coil will be tens of thousands or hundreds of thousands of amperes. No AC power system normally operates at these current levels and hence a transformer is mounted on each side of the converter unit to convert the high voltage and low current of the AC system to the low voltage and high current required by the coil. The energy exchange between the superconducting coil and the electric power system is controlled by a line commutated converter. To reduce the harmonics produced on the AC bus and in the output voltage to the coil, a 12-pulse converter is preferred. The superconducting coil can be charged to a set value from the grid during normal operation of the power system. Once the superconducting coil gets charged, it conducts current with virtually no losses [11–16] as the coil is maintained at extremely low-temperatures. When there is a sudden rise in the load demand, the stored energy is almost released through the PCS to the power system as alternating current. As the governor and other control mechanisms start working to set the power system to the new equilibrium condition, the coil current changes back to its initial value. Similar action occurs during sudden release of loads. In this case, the coil immediately gets charged towards its full value, thus absorbing some portion of the excess energy in the system and as the system returns to its steady state, the excess energy absorbed is released and the coil current attains its normal value. The control of the converter firing angle provides the DC voltage appearing across the inductor to be continuously varying within a certain range of positive and

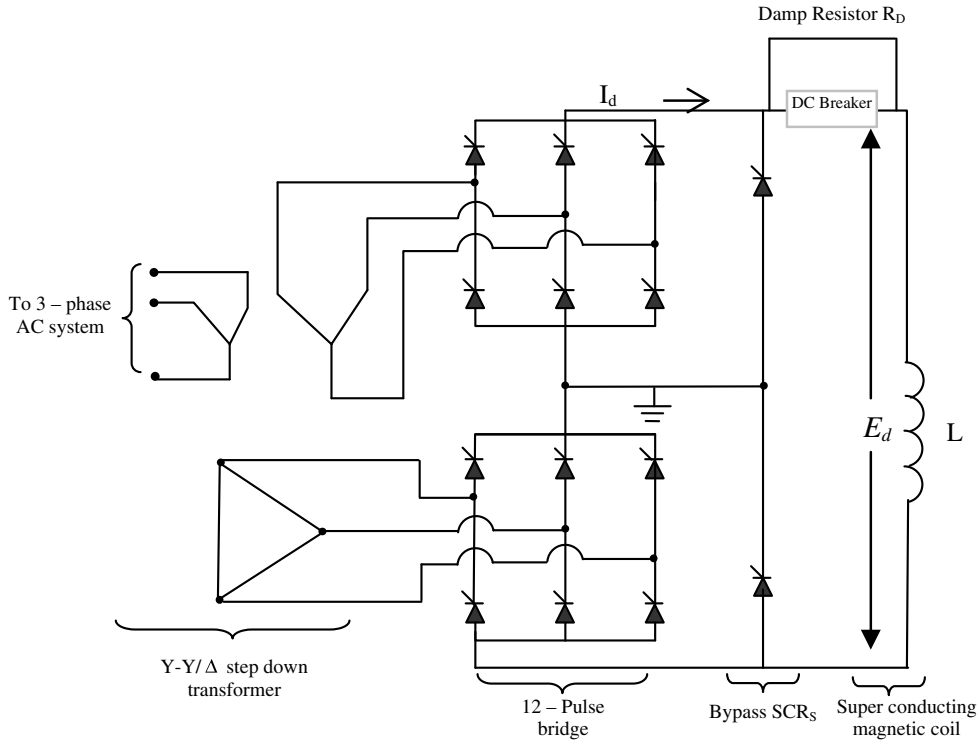

Fig. 1. SMES circuit diagram.

negative values. The inductor is initially charged to its rated current I_{d0} by applying a small positive voltage. Once the current reaches its rated value, it is maintained constant by reducing the voltage across the inductor to zero since the coil is superconducting. Neglecting the transformer and the converter losses, the DC voltage is given by [15]

$$E_d = 2V_{d0}\cos\alpha - 2I_dR_C \tag{1}$$

where E_d is the DC voltage applied to the inductor in kV, α is the firing angle in degrees, I_d is the current flowing through the inductor in kA, R_C is the equivalent commutating resistance in kΩ and V_{d0} is the maximum circuit bridge voltage in kV. Charging and discharging of the SMES unit is controlled through the change of commutation angle α. If α is less than 90°, converter acts in the converter mode (charging mode) and if α is greater than 90°, the converter acts in the inverter mode (discharging mode).

In LFC operation, the E_d is continuously controlled by the input signal to the SMES control logic. As mentioned in recent literatures [11–16], the inductor current must be restored to its nominal value quickly after a system disturbance so that it can respond to the next load disturbances immediately. Thus, in order to improve the current restoration to its steady state value the inductor current deviation is used as a negative feedback signal in the SMES control loop. Based on the above dissuasion, the converter voltage applied to the inductor and inductor current deviations are described as follows:

$$\Delta E_{di}(s) = \frac{K_{SMES}}{1+sT_{dci}}u_{SMESi}(s) - \frac{K_{id}}{1+sT_{dci}}\Delta I_{di}(s) \tag{2}$$

$$\Delta I_{di}(s) = \frac{1}{sL_i}\Delta E_{di}(s) \tag{3}$$

In this study, as in recent literatures, the input signal to the SMES control logic is considered the ACE_i of the same area in power system [9]. The ACE_i is defined as follows:

$$ACE_i = B_i\Delta F_i + \Delta P_{tie,i} \tag{4}$$

The deviation in the inductor real power of SMES unit is expressed in time domain as follows:

$$\Delta P_{SMESi} = \Delta E_{di}I_{d0i} + \Delta I_{d0i}\Delta E_{di} \tag{5}$$

This value is assumed positive for transfer from AC grid to DC. Fig. 2 shows the block diagram of SMES unit.

3. Description of generalized LFC scheme

In the deregulated power systems, the vertically integrated utility no longer exists. However, the common LFC objectives, i.e. restoring the frequency and the net interchanges to their desired values for each control area, still remain. The deregulated power system consists of GENCOs, TRANSCOs and DISCOs with an open access policy. In the new structure, GENCOs may or may not participate in the LFC task and DISCOs have the liberty to contract with any available GENCOs in their own or other areas. Thus various combinations of possible contracted scenarios between DISCOs and GENCOs are possible. All the transactions have to be cleared by the independent system operator (ISO) or other responsible organizations. In this new environment, it is desirable that a new model for LFC scheme be developed to account for the effects of possible load following contracts on system dynamics.

Based on the idea presented in [17], the concept of an '*Augmented Generation Participation Matrix*' (AGPM) to express the possible contracts following is presented here. The AGPM shows the participation factor of a GENCO in the load following contract with a DISCO. The rows and columns of AGPM matrix equal the total number of GENCOs and DISCOs in the overall power system, respectively. Consider the number of GENCOs and DISCOs in area i be n_i and m_i in a large scale power system with N control areas. The structure of AGPM is given by

$$\mathrm{AGPM} = \begin{bmatrix} \mathrm{AGPM}_{11} & \cdots & \mathrm{AGPM}_{1N} \\ \vdots & \ddots & \vdots \\ \mathrm{AGPM}_{N1} & \cdots & \mathrm{AGPM}_{NN} \end{bmatrix} \tag{6}$$

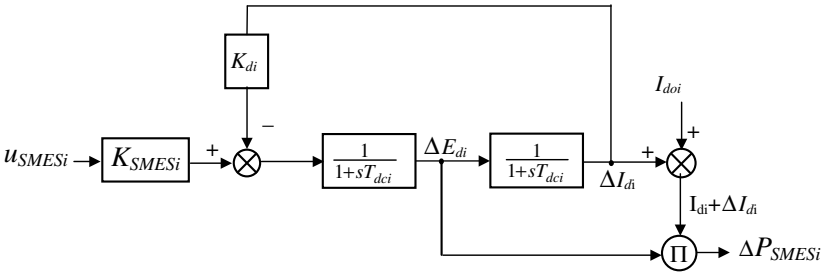

Fig. 2. The block diagram of SMES unit.

where

$$\mathrm{AGPM}_{ij} = \begin{bmatrix} gpf_{(s_i+1)(z_j+1)} & \cdots & gpf_{(s_i+1)(z_j+m_j)} \\ \vdots & \ddots & \vdots \\ gpf_{(s_i+n_i)(z_j+1)} & \cdots & gpf_{(s_i+n_i)(z_j+m_j)} \end{bmatrix}$$

For $i,j = 1,\ldots,N$ and

$$s_i = \sum_{k=1}^{i-1} n_i, z_j = \sum_{k=1}^{j-1} m_j \quad \text{and} \quad s_1 = z_1 = 0$$

In the above, gpf_{ij} refers to '*generation participation factor*' and shows the participation factor of GENCO i in total load following requirement of DISCO j based on the contracted scenario. Sum of all entries in each column of AGPM is unity. The diagonal sub-matrices of AGPM correspond to local demands and off-diagonal sub-matrices correspond to demands of DISCOs in one area on GENCOs in another area.

Block diagram of the generalized LFC scheme in a restructured system is shown in Fig. 3 with considering SMES unit. Dashed lines show interfaces between areas and the demand signals based on the possible contracts. These new information signals are absent in the traditional LFC scheme. As there are many GENCOs in each area, ACE signal has to be distributed among them due to their ACE participation factor in the LFC task and $\sum_{j=1}^{n_i} \alpha_{ji} = 1$.

Fig. 4 shows the modified LFC scheme for control area i in a restructured system. It can be seen from this figure that four input disturbance channels, d_i, η_i, ζ_i and ρ_i are considered for decentralized LFC design. They are defined as below

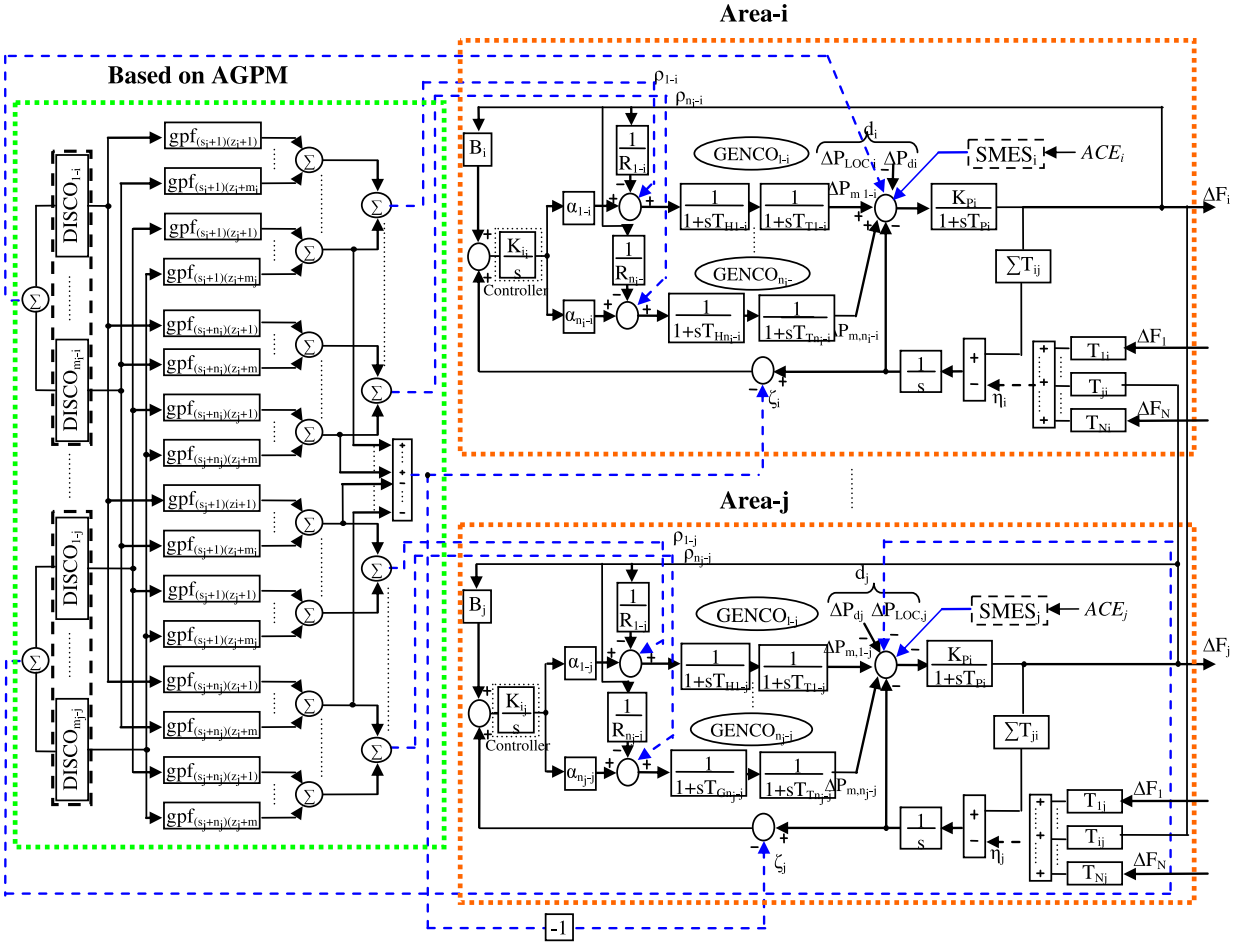

Fig. 3. The generalized LFC scheme in the restructured system.

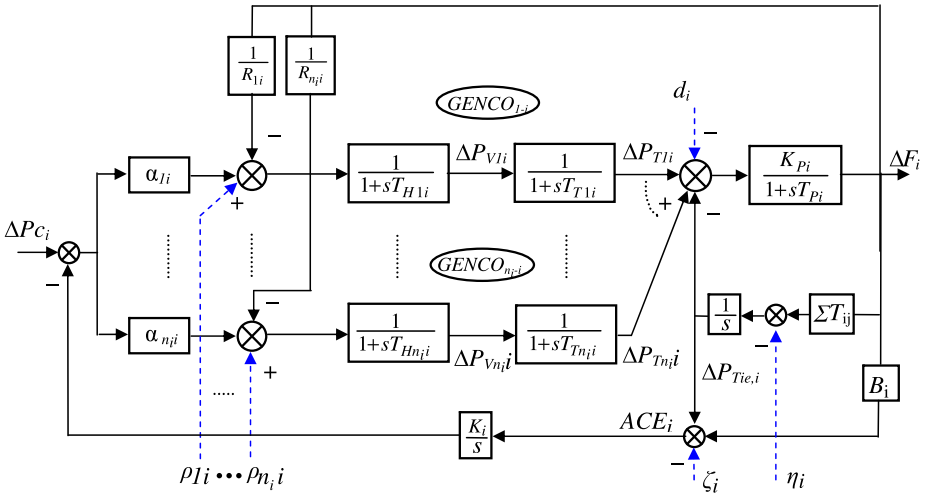

Fig. 4. The decentralized LFC scheme for area i in the restructured environment.

$$d_i = \Delta P_{\mathrm{Loc},i} + \Delta P_{di}, \quad \Delta P_{\mathrm{Loc},i} = \sum_{j=1}^{m_i} (\Delta P_{Lj} + \Delta P_{ULj}) \tag{7}$$

$$\eta_i = \sum_{\substack{j=1 \\ j\neq i}}^{N} T_{ij}\Delta f_j \tag{8}$$

$$\zeta_i = \Delta P_{\mathrm{tie},i,\mathrm{sch}} = \sum_{\substack{k=1 \\ k\neq i}}^{N} \Delta P_{\mathrm{tie},ik,\mathrm{sch}} \tag{9}$$

$$\Delta P_{\mathrm{tie},ik,\mathrm{sch}} = \sum_{j=1}^{n_i}\sum_{t=1}^{m_k} apf_{(s_i+j)(z_k+t)}\Delta P_{L(z_k+t)} - \sum_{t=1}^{n_k}\sum_{j=1}^{m_i} apf_{(s_k+t)(z_i+j)}\Delta P_{L(z_i+j)} \tag{10}$$

$$\Delta P_{\mathrm{tie},i-\mathrm{error}} = \Delta P_{\mathrm{tie},i-\mathrm{actual}} - \zeta_i \tag{11}$$

$$\rho_i = [\rho_{1i}\cdots\rho_{ki}\cdots\rho_{n_i i}]^{\mathrm{T}}, \quad \rho_{ki} = \sum_{j=1}^{N}\left[\sum_{t=1}^{m_j} gpf_{(s_i+k)(z_j+t)}\Delta P_{Lt-j}\right] \tag{12}$$

$$\Delta P_{m,k-i} = \rho_{ki} + apf_{ki}\sum_{j=1}^{m_i}\Delta P_{ULj-i} \tag{13}$$

$\Delta P_{m,ki}$ is the desired total power generation of a GENCO k in area i and must track the demand of the DISCOs in contract with it in the steady state.

Due to Fig. 4, the state-space model for control area i can be obtained as

$$\begin{aligned} \dot{x}_i &= A_i x_i + B_{iu}u + B_{iw}w_i' \\ y_i &= C_i x_i + D_{iw}w_i' \end{aligned} \tag{14}$$

where

$$x_i^{\mathrm{T}} = [x_{ai}x_{1i}\cdots x_{ki}\cdots x_{n_i i}], \quad u_i = \Delta P_{ci}, \quad y_i = \mathrm{ACE}_i$$

$$x_{ai} = [\Delta f_i \Delta P_{\mathrm{tie},i}\int \mathrm{ACE}_i], \quad x_{ki} = [\Delta P_{Tki}\Delta P_{Vki}], \quad k = 1,\ldots,n_i$$

$$w_i'^{\mathrm{T}} = [\,\Delta P_{\mathrm{Loc},i} \quad \eta_i \quad \xi_i \quad \rho_i\,], \quad \rho_i = [\rho_{1i}\cdots\rho_{ki}\cdots\rho_{n_i i}]$$

$$A_i = \begin{bmatrix} A_{11i} & A_{12i} \\ A_{21i} & A_{22i} \end{bmatrix}, \quad A_{11i} = \begin{bmatrix} 1/T_{Pi} & -K_{Pi}/T_{Pi} & 0 \\ \sum_{j=1\&j\neq i}^{N} T_{ji} & 0 & 0 \\ B_i & 1 & 0 \end{bmatrix}$$

$$A_{12i} = \underbrace{\left[\begin{pmatrix} K_{Pi}/T_{Pi} & 0 & 0 \\ 0 & 0 & 0 \\ 0 & 0 & 0 \end{pmatrix} \cdots \begin{pmatrix} K_{Pi}/T_{Pi} & 0 & 0 \\ 0 & 0 & 0 \\ 0 & 0 & 0 \end{pmatrix}\right]}_{n_i \text{blocks}}$$

$$A_{21i} = [DP_{1i}^{\mathrm{T}}\cdots DP_{ki}^{\mathrm{T}}\cdots DP_{n_i i}^{\mathrm{T}}],$$

$$A_{22i} = \mathrm{diag}(TG_{1i},\ldots,TG_{ki},\ldots,TG_{n_i i})$$

$$DP_{ki} = \begin{bmatrix} 0 & 0 & 0 \\ -1/(R_{ki}T_{Hki}) & 0 & -K_i\alpha_{ki}/T_{Hki} \end{bmatrix},$$

$$TG_{ki} = \begin{bmatrix} -1/T_{Tki} & 1/T_{Tki} \\ 0 & -1/T_{Hki} \end{bmatrix} \quad B_{iu}^{\mathrm{T}} = [0_{3\times1}^{\mathrm{T}} \quad B_{1iu}^{\mathrm{T}}\cdots B_{kiu}^{\mathrm{T}}\cdots B_{n_i iu}^{\mathrm{T}}],$$

$$B_{kiu} = [0 \quad \alpha_{ki}/T_{Hki}] \quad B_{iw}^{\mathrm{T}} = [B_{aiw}^{\mathrm{T}} \quad B_{1iw}^{\mathrm{T}}\cdots B_{kiw}^{\mathrm{T}}\cdots B_{n_i iw}^{\mathrm{T}}]$$

$$B_{aiw} = \begin{bmatrix} -K_{Pi}/T_{Pi} & 0 & 0 & 0_{1\times n_i} \\ 0 & -1 & 0 & 0_{1\times n_i} \\ 0 & 0 & -1 & 0_{1\times n_i} \end{bmatrix}$$

$$B_{kiw} = \begin{bmatrix} 0_{1\times3} & 0\cdots0\cdots0 \\ 0_{1\times3} & b_{1i}\cdots b_{ki}\cdots b_{n_i i} \end{bmatrix}, \; b_{ji} = \begin{cases} -1/T_{Hki} & j = k \\ 0 & j \neq i \end{cases}$$

$$C_i = [C_{ai} \quad 0_{1\times2n_i}], \quad C_{ai} = [\,B_i \quad 1 \quad 0\,], \quad D_{iw} = [\,0_{1\times2} \quad -1 \quad 0_{1\times n_i}\,]$$

4. Mixed H_2/H_∞ and the proposed control framework

This section gives a technical background about the mixed H_2/H_∞ control technique. Also, the proposed synthesis methodology for LFC problem based on the mixed H_2/H_∞ control is given.

4.1. Mixed H_2/H_∞: technical background

In many real world control application, multi-objectives such as stability, disturbance attenuation and reference tracking under model uncertainties and practical constraints are followed simultaneously. On the other hand, each robust control method is mainly useful to capture a set of special design specifications. For instance, noise attenuation or regulation against random disturbances is more naturally expressed in LQG terms (H_2 synthesis). Similarly, pure H_∞ synthesis is more useful for holding close loop stability and formulation of some uncertainties and practical control constraints. It is shown that combination of H_2 and H_∞ (mixed H_2/H_∞) control techniques gives a powerful multi-objectives design including both sets of the above objectives [7,8]. The synthesis problem is shown in Fig. 5. $P(s)$ is a linear time invariant system with the following state-space realization:

$$\begin{aligned} \dot{x} &= Ax + B_1 w + B_2 u \\ z_\infty &= C_\infty x + D_{\infty 1} w_i + D_{\infty 2} u \\ z_2 &= C_2 x + D_{21} w_i + D_{22} u_i \\ y_i &= c_y x + D_{y1} w_i \end{aligned} \tag{15}$$

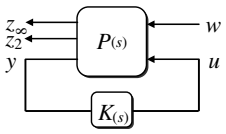

Fig. 5. The mixed H_2/H_∞ synthesis structure.

where x is the state variable vector, w is the disturbance and other external vector and y is the measured output vector. The output channels z_∞ is associated with the H_∞ performance, while the output channel z_2 is associated with the H_2 performance.

Denoting by $T_\infty(s)$ and $T_2(s)$, the transfer functions from w to z_∞ and z_2, respectively, the mixed H_2/H_∞ synthesis problem can be expressed by the following optimization problem: design a controller $K(s)$ that minimize a trade off criterion of the form:

$$\alpha\|T_\infty(s)\|^2 + \beta\|T_2(s)\|^2 \qquad (\alpha\&\beta \geqslant 0) \tag{16}$$

An efficient algorithm for solving this problem is available in LMI control toolbox of MATLAB [18]. The following lemmas relate the above optimization control problem to LMI techniques. Assume that the state-space realization of close loop system is given by as

$$\begin{aligned} \dot{x}_{cl} &= A_{c1}x_{c1} + B_{c1}w \\ z_\infty &= C_{cl\infty}x_{cl} + D_{cl\infty}w \\ z_2 &= C_{cl2}x_{cl} + D_{cl2}w \end{aligned} \tag{17}$$

Lemma 1. (H_∞ *performance*) [8] *The closed loop RMS gain for $T_\infty(s)$ does not exceed γ_∞ if and only if there exist a symmetric matrix $X_\infty > 0$ such that*

$$\begin{bmatrix} A_{cl}X_\infty + X_\infty A_{cl}^{\mathrm{T}} & B_{cl} & X_\infty C_{cl}^{\mathrm{T}} \\ B_{cl}^{\mathrm{T}} & -I & D_{cl\infty}^{\mathrm{T}} \\ C_{cl\infty}X_\infty & D_{cl\infty} & -\gamma_\infty^2 I \end{bmatrix} < 0 \tag{18}$$

Lemma 2. (H_2 *performance*)[8] *The H_2 norm of $T_2(s)$ does not exceed γ_2 if and only if $D_{cl2} = 0$ and here exist two symmetric matrices X_2 and Q such that*

$$\begin{bmatrix} A_{cl}X_2 + X_2A_{cl}^{\mathrm{T}} & B_{cl} \\ B_{cl}^{\mathrm{T}} & -I \end{bmatrix} < 0, \begin{bmatrix} Q & C_{cl2}X_2 \\ X_2C_{cl2}^{\mathrm{T}} & X_2 \end{bmatrix} > 0, \quad \mathrm{trace}(Q) < \gamma_2^2 \tag{19}$$

4.2. LFC problem formulation via mixed H_2/H_∞

LFC goals, i.e. frequency regulation and tracking the load demands, maintaining the tie-line power interchanges to specified values in the presence of modeling uncertainties, system nonlinearities and area load disturbances determines the LFC synthesis as a multi-objective optimization problem. For this reason, the idea of mixed H_2/H_∞ control synthesis, which gives a powerful multi-objectives design is used for the solution this problem. The main synthesis framework to formulate it as a mixed H_2/H_∞ control design for a given control area (Fig. 4) is shown in Fig. 6.

In the power systems, each control area contains different kinds of uncertainties because of plant parameter variations, load changes and system modeling errors due to some approximations in model linearization and un-modeled dynamics. Usually, the uncertainties in power system can be modeled as multiplicative and/or additive uncertainties [19]. In Fig. 6 the Δu_i block models the structured uncertainties as a multiplicative type and W_{ui} is the associated weighting function. The output channels $z_{\infty i,1}$ and $z_{\infty i,2}$ are associated with H_∞ performance. The first channel is used to meet robustness against uncertainties and reduce their impacts on close loop system performance. In the second channel ($z_{\infty i,2}$) W_{Ci} sets a limit on the allowed control signal to penalize fast change and large overshoot in the control action signal with regard to practical constraints. The output channel z_{2i} is associated with the H_2 performance and W_{Pi} sets the performance goal, i.e. zero tracking error and minimizing the effects of disturbances on the area control error (ACE_i). We can redraw the Fig. 6 as a mixed H_2/H_∞ general framework synthesis as shown in Fig. 7, where $P_{oi}(s)$ and $K_i(s)$ denote the nominal area model as given by Eq. (16) and controller, respectively. Also, y_i is the measured output (performed by ACE_i), u_i is the control output and w_i includes the perturbed, disturbance and reference signals in the control area.

In Fig. 7, $P_i(s)$ is the generalized plant (GP) that includes nominal models of control area i and associated weighting functions. The state-space model of GP can be obtained as

$$\begin{aligned} \dot{x}_{\mathrm{GP}i} &= A_{\mathrm{GP}i}x_{\mathrm{GP}i} + B_{1i}w_i + B_{2i}u_i \\ z_{\infty i} &= C_{\infty i}x_{\mathrm{GP}i} + D_{\infty 1i}w_i + D_{\infty 2i}u_i \\ z_{2i} &= C_{2i}x_{\mathrm{GP}i} + D_{21i}w_i + D_{22i}u_i \\ y_i &= c_{yi}x_{\mathrm{GP}i} + D_{y1i}w_i \end{aligned} \tag{20}$$

where

$$w_i^{\mathrm{T}} = [v_i \quad d_i \quad \eta_i \quad \zeta_i \quad \rho_i \quad y_{ref}], \quad z_{\infty i}^{\mathrm{T}} = [z_{\infty 1i} \quad z_{\infty 2i}]$$

Now, the synthesis problem is designing a controller $K_i(s)$ as shown in Fig. 7 such that Eq. (16) is minimized. It is should be noted that the order of found controller by this strategy is the same as size of generalized plant that is typically high in general. In order to overcome the complexity of computation in the case of high order power systems, appropriated model reduction techniques might be applied to the obtained controller model. In summary, the designing steps of the proposed method are

Step 1: Formulation of the LFC problem as a decentralized control scheme due to Fig. 4 and identify the state-space model for the given control area.

Step 2: Identify the uncertainty (W_{ui}) and performance weighting functions (W_{Pi} and W_{Ci}) for the given area according to dynamical model, practical limits and performance requirements.

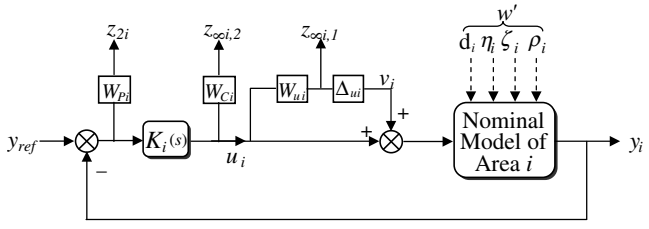

Fig. 6. The proposed synthesis framework.

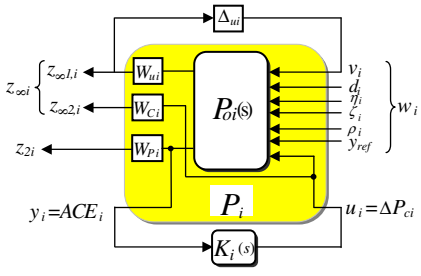

Fig. 7. The formulation of mixed H_2/H_∞ based control design problem.

Step 3: Problem formulation as a general mixed H_2/H_∞ control structure according to Fig. 7.
Step 4: Identify the indexes α, β and solve optimization problem Eq. (16) using LMI approaches to obtain desired controller.
Step 5: Reduce the order of result controller by using standard model reduction techniques.
Step 6: Continue this procedure by applying the above steps to other control area.

The proposed control methodology in this paper includes enough flexibility to set the desired level of robust performance and provides a set of robust decentralized controllers which guarantee stability of the overall power system. On the other hand, it has a decentralized scheme and requires only the ACE in each control area. Thus, its construction and implementation are easy and can be useful in the real world complex power system.

5. Case study

A four-area power system considering two SMES units in areas 1 and 3, shown in Fig. 8 is considered as a test system to demonstrate the effectiveness of the proposed control strategy. It is assumed that each control area includes two GENCOs and two DISCOs except areas two and four have one DISCO. The system parameters are the same as [20] and given in Appendix.

Simulation results and eigenvalue analysis show that the open loop system performance is affected more significantly by changing in the K_{pi}, T_{pi}, B_i and T_{ij} than changes of other parameters. Thus, to illustrate the capability of the proposed strategy in this example, in the view point of uncertainty our focus will be concentrated on variation of these parameters. Hence, for the given power system, we have set our objectives to area frequency regulation and assuring robust stability and performance in the presence of specified uncertainties, load changes and contract variations as follows:

1. Holding stability and robust performance for the overall power system and each control area in the presence of 25% uncertainty for the K_{pi}, T_{pi}, B_i and T_{ij}.
2. Minimizing the effects of new introduced disturbances on the output signals according to the possible contracts.
3. Getting zero steady state error and good tracking for load demands and disturbances.
4. Maintaining acceptable overshoot and settling time on the frequency deviation signal in each control area.
5. Setting the reasonable limit on the control action signal from the change speed and amplitude view point.

In the following subsection, we will discuss application of the proposed strategy on the given power system to achieve the above objectives for each of the four control areas separately. Because of similarity and to save space, the first controller synthesis will be described in detail and for the other control areas, only the final results would be presented.

5.1. Weighting functions selection

5.1.1. Uncertainty weights selection

As it is mentioned in the previous section, we can consider the specified uncertainty in each area as a multiplicative uncertainty associated with a nominal model. Let $\widehat{P}_i(s)$ denote the transfer function from the control input u_i to control output y_i at operating points other than the nominal point. Following a practice common in robust control, this transfer can be represented as

$$\begin{aligned} &|\Delta u_i(s) W_i(s)| = |(\widehat{P}_i(s) - P_{oi}(s))/P_{oi}(s))|; \quad P_{oi}(s) \neq 0 \\ &\|\Delta u_i(s)\|_\infty = \sup |\Delta u_i(s)| \leqslant 1 \end{aligned} \tag{21}$$

where $\Delta u_i(s)$ shows the uncertainty block corresponding to the uncertain parameters and $P_{oi}(s)$ is the nominal transfer function model. Thus, $W_{ui}(s)$ is such that its magnitude Bode plot covers the Bode plot of all possible plants. Using Eq. (21) some sample uncertainties corresponding to different values of K_{pi}, T_{pi}, B_i and T_{ij} are shown in Fig. 9 for one area. It can be seen that multiplicative uncertainties have a peak around the 6.5 rad/s. Based on this figure the following multiplicative uncertainty weight was chosen for control design as:

$$W_{u1} = \frac{16.13s^2 + 26.22s + 21.33}{s^2 + 0.9s + 44.07} \tag{22}$$

Fig. 9 clearly shows that attempting to cover the sharp peak around the 6.5 rad/s will result in large gaps between the weight and uncertainty at other frequencies. On the other hand, a tighter

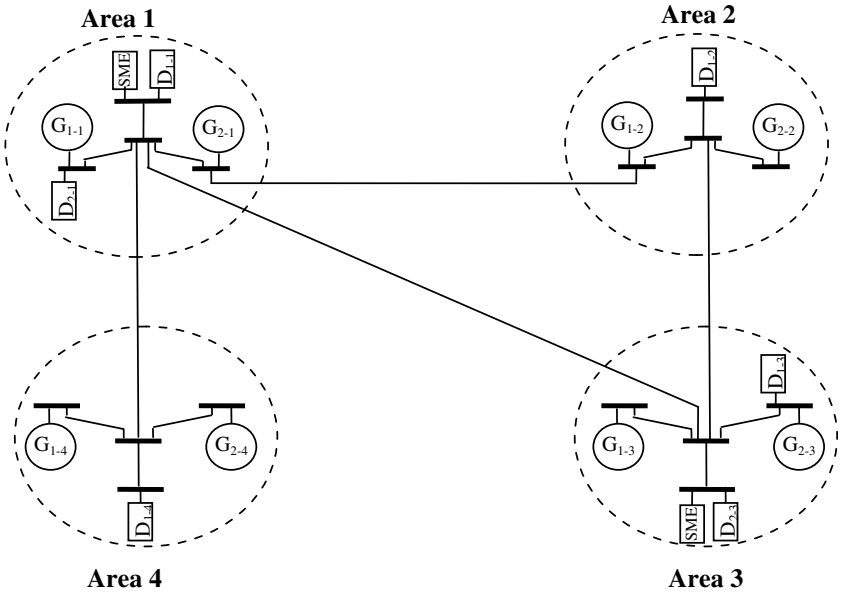

Fig. 8. Four-area control power system.

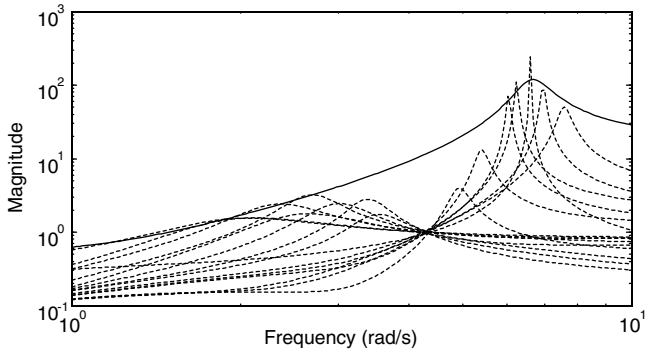

Fig. 9. Uncertainty plot due to change of K_{p1}, T_{p1}, B_1 and T_{j1} (dashed) and $W_{u1}(s)$ (solid).

fit at all frequencies using a high order transfer function will result in a high order controller. The weight (22) used in our design give a conservative design at around the 6.5 rad/s, low and high frequencies, but it provides a good trade off between robustness and controller complexity. Using the same method, the uncertainty weighting function for area 2, 3 and 4 are calculated as follows:

$$W_{u2} = \frac{19.7s^3 + 17.32s^2 + 232.1s + 53.29}{s^3 + 4.49s^2 + 41s + 148.2}$$
$$W_{u3} = \frac{68s^3 + 154.9s^2 + 1343.7s + 1246}{s^3 + 31.16s^2 + 84.7s + 1159} \quad (23)$$
$$W_{u4} = \frac{1666s^3 + 3510s^2 + 31414s + 25311}{s^3 + 1150s^2 + 1364.1s + 36489}$$

5.1.2. Performance weights selection

The selection of performance weights W_{Ci} and W_{Pi} entails a trade off among different performance requirements, particularly good area control error minimization versus peak control action. The weight on the control input, W_{Ci}, must be chosen close to a differentiator to penalize fast change and large overshoot in the control input due to corresponding practical constraints. The weight on the output, W_{Pi}, must be chosen close to an integrator at low frequency in order to get disturbance rejection and zero steady state error. More details on how these weights are chosen are given in [21–23]. Based on the above discussion, a suitable set of performance weighting functions for one control area is chosen as

$$W_{C1} = \frac{0.1s}{83(0.001s + 1)}, \quad W_{P1} = \frac{0.04s + 0.8}{150s + 1} \quad (24)$$

5.2. Mixed H_2/H_∞ control design

Based on the problem formulation and synthesis methodologies in Section 4, a decentralized robust controller is designed for one control area using the *hinfmix* function in the LMI control toolbox. This function gives an optimal controller through the mentioned optimization problem Eq. (16) with α and β fixed at unity. The resulting controller is dynamic type and whose order is the same as the size of the GP model (here 11). The order of controller is reduced to a four with no performance degradation using the standard Hankel norm approximation. The Bode plots of the full order and reduced order controllers are shown in Fig. 10. The transfer function of the reduced order controller with simple structure is given as

$$K_1(s) = -9.86 \times 10^{-3} \times \frac{s^5 + 9.97s^4 + 33.3s^3 + 121.59s^2 + 47.7s + 1.59}{s^6 + 3.87s^5 + 9.44s^4 + 10.87s^3 + 8.35s^2 + 2.67s + 0.067} \quad (25)$$

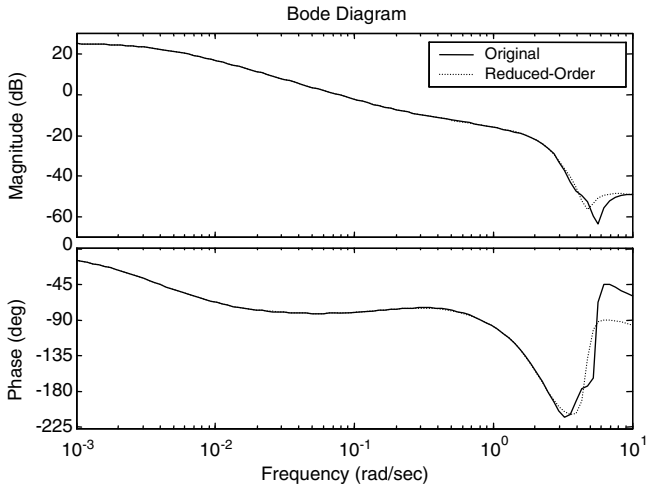

Fig. 10. Bode plot comparison of original and reduced order controller $K_1(s)$.

Table 1
Performance weighting functions

Weight	Area-2	Area-3	Area-4
W_{Pi}	$\frac{0.05s}{83(0.001s+1)}$	$\frac{0.04s}{63(0.01s+1)}$	$\frac{0.03s}{93(0.001s+1)}$
W_{Ci}	$\frac{0.01s+0.5}{280s+1}$	$\frac{0.01s+0.4}{300s+1}$	$\frac{0.01s+0.8}{480s+1}$

Using the same procedure and setting similar objectives as discussed above the set of suitable weighting function for the other control area synthesizes are given in Table 1. The resulting controllers can be approximated by low order controllers as follows:

$$K_2(s) = -1.03 \times 10^{-2} \frac{s^5 + 12.93s^4 + 52.27s^3 + 226.5s^2 + 801.46s + 1.03}{s^6 + 3.51s^5 + 15.9s^4 + 25.6s^3 + 14.85s^2 + 3.02s + 0.011}$$
$$K_3(s) = 5.14 \times 10^{-3} \frac{s^4 - 8.72s^3 + 17.57s^2 - 148.82s - 4.01}{s^5 + 1.89s^4 + 21.42s^3 + 32.42s^2 + 22.96s + 0.077}$$
$$K_4(s) = -4.4 \times 10^{-3} \frac{s^4 - 32.3s^3 - 73.03s^2 - 1151.25s + 24.59}{s^5 + 5.45s^4 + 22.68s^3 + 35.15s^2 + 15.74s + 0.034} \quad (26)$$

6. Simulation results

In the simulation study, the linear model of turbine $\Delta PV_{ki}/\Delta PT_{ki}$ in Fig. 3 is replaced by a nonlinear model of Fig. 11 (with ±0.05 limit). This is to take GRC into account, i.e. the practical limit on the rate of the change in the generating power of each GENCO. The results in Ref. [16,21] indicated that GRC would influence the dynamic responses of the system significantly and lead to larger overshot and longer settling time. Moreover, from the point view of economy SMES unit is considered only in one and three areas of the power system [15]. Thus, affirmative effect of SMES on LFC is also taken into account in the study. The effect of SMES in the improvement of LFC at power systems is known in the literatures.

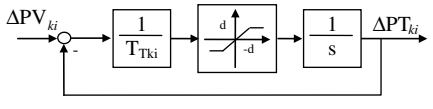

Fig. 11. Nonlinear turbine model with GRC.

The close loop system performance using the proposed controllers in comparison with the conventional PI controllers (which is widely used for LFC problem in industry) is tested for two cases of operating conditions in the presences of load demands, disturbances and uncertainties. In addition, during operation, both the effects of SMES and mixed H_2/H_∞ controller are investigated together.

6.1. Scenario 1

In this scenario, the closed loop performance is tested in the presence of both step contracted load demands and uncertainties. It is assumed that a large step load is demanded by all DISCOs as follow:

$$\Delta P_{L1-1} = 100, \quad \Delta P_{L2-1} = 50, \quad \Delta P_{L1-2} = 100,$$
$$\Delta P_{L1-3} = 80, \quad \Delta P_{L2-3} = 60, \quad \Delta P_{L1-4} = 100 \text{ MW}$$

A case of combined Poolco and bilateral based contracts between DISCOs and available GENCOs is considered based on the following AGPM:

$$\text{AGPM}^{\text{T}} = \begin{bmatrix} 0.4 & 0 & 0.4 & 0 & 0.2 & 0 & 0 & 0 \\ 0 & 0.2 & 0 & 0.4 & 0 & 0 & 0 & 0.4 \\ 0 & 0 & 0.4 & 0 & 0 & 0.6 & 0 & 0 \\ 0 & 0.4 & 0 & 0.2 & 0.4 & 0 & 0 & 0 \\ 0.8 & 0 & 0 & 0 & 0 & 0.2 & 0 & 0 \\ 0 & 0 & 0 & 0 & 0 & 0 & 0.5 & 0.5 \end{bmatrix}$$

All GENCOs participate in the LFC task. The one GENCO in area 4 only participate for performing the LFC in its area, while other GENCOs track the load demand in their areas and/or others. Power system responses with 25% increase in uncertain parameters K_{Pi}, T_{Pi}, B_i and T_{ij} are depicted in Figs. 12 and 13 without and with SMES unit, respectively. Using the proposed method and considering SMES unit, the frequency deviation of all areas is quickly driven back to zero and the tie-line power flows properly converges to the specified values of Eq. (10) in the steady state, i.e.

$$\Delta P_{\text{tie},1,\text{sch}} = -0.02, \quad \Delta P_{\text{tie},2,\text{sch}} = 0.016, \quad \Delta P_{\text{tie},3,\text{sch}} = -0.016,$$
$$\Delta P_{\text{tie},4,\text{sch}} = 0.02 \text{ pu MW}$$

6.2. Scenario 2

In this case, a DISCO may violate a contract by demanding more power than that specified in the contract. This excess power is reflected as a local load of the area (un-contracted load). Consider scenario 1 again. It is assumed that in addition to specified contracted load demands and 25% decrease in uncertain parameters, the one DISCO from areas 1 and 3 demand 0.1 and 0.06 pu MW as a large un-contracted load, respectively. Using the Eq. (7), the total local load in all areas is obtained as

$$\Delta P_{\text{Loc},1} = 0.25, \quad \Delta P_{\text{Loc},2} = 0.16, \quad \Delta P_{\text{Loc},3} = 0.14,$$
$$\Delta P_{\text{Loc},4} = 0.1 \text{ pu MW}$$

The purpose of this scenario is to test the effectiveness of the proposed controller against uncertainties and large load disturbances in the presence of GRC. The power system responses are shown in Figs. 14 and 15 without and with SMES unit. Using the proposed method and considering SMES, the frequency oscillation is quickly driven damped and the tie-line power flows properly converge to the specified value of Eq. (10) in the steady state. As AGPM is the same as in scenario 1 and the un-contracted load of areas is taken up by the GENCOs in the same areas, the tie-line power is the same as in scenario 1 in the steady state. The un-contracted load of DISCOs in area 1 and 3 is taken up by the GENCOs in these areas according to ACE participation factors in the steady state.

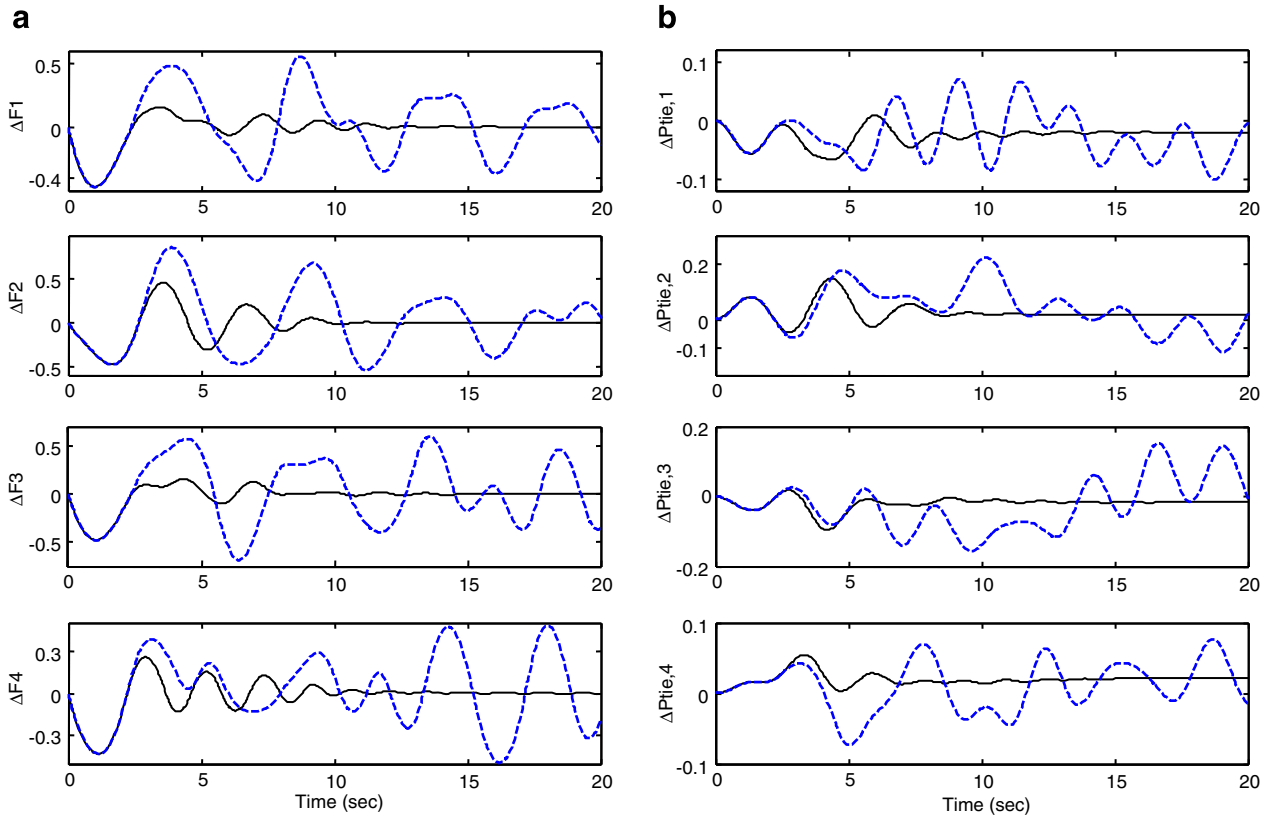

Fig. 12. Power system responses to scenario 1 without SMES unit: (a) Frequency deviation and (b) tie-line power changes; solid (mixed H_2/H_∞) and dashed (PI).

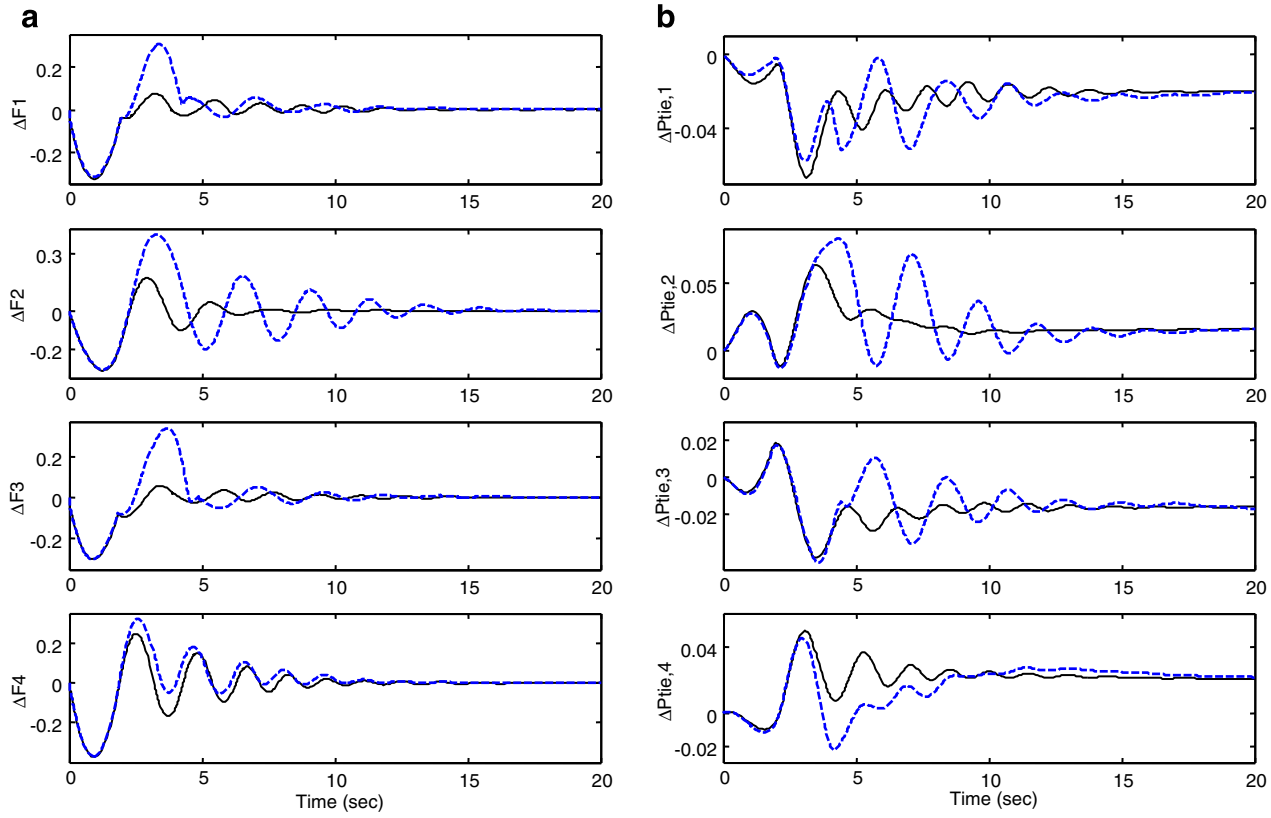

Fig. 13. Power system responses to scenario 1 with SMES unit: (a) frequency deviation and (b) tie-line power changes; solid (mixed H_2/H_∞) and dashed (PI).

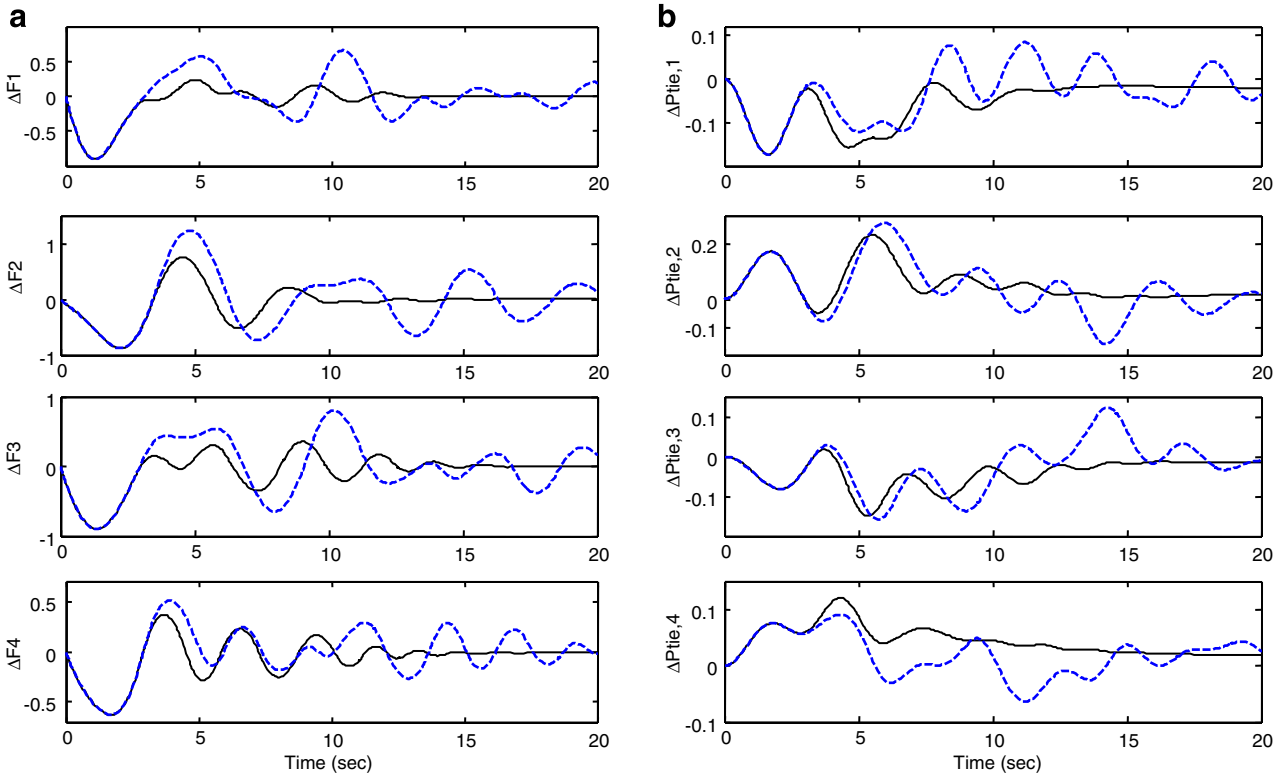

Fig. 14. Power system responses to scenario 2 without SMES unit: (a) frequency deviation and (b) tie-line power changes; solid (mixed H_2/H_∞) and dashed (PI).

The simulation results in the above scenarios indicate that the proposed control strategy can ensure the robust performance such as frequency tracking and disturbance attenuation for possible contracted scenarios under modeling uncertainties and large area load demands in the presence of GRC. Moreover, the simulations represent the positive effect of SMES unit on the improvement of

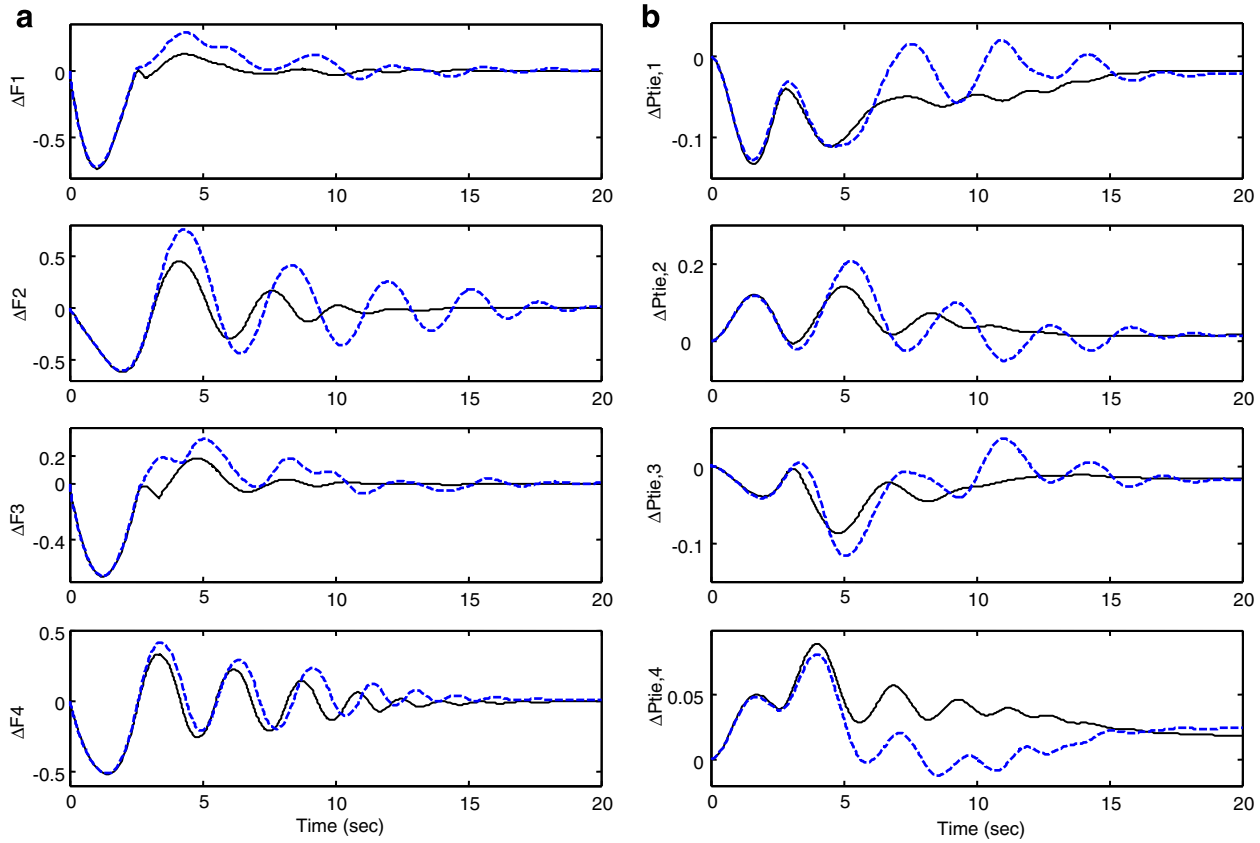

Fig. 15. Power system responses to scenario 2 with SMES unit: (a) frequency deviation (b) tie-line power changes; solid (mixed H_2/H_∞) and dashed (PI).

Table 2
ITAE values with the mixed H_2/H_∞ and PI controllers

Test No.	Parameter change (%)	Scenario 1				Scenario 2			
		With SMES		Without SMES		With SMES		Without SMES	
		Mixed	PI	Mixed	PI	Mixed	PI	Mixed	PI
1	−25	27.3	50.9	61.3	224.6	126.1	198.7	199.2	596.1
2	−20	28.7	56.3	67.5	245.6	131.1	199.2	210.0	710.0
3	−15	30.2	61.7	73.5	274.5	137.0	178.3	219.4	818.7
4	−10	31.8	67.1	79.1	401.7	143.8	157.7	234.3	886.5
5	−5	33.4	71.2	84.3	519.6	151.1	164.8	256.6	956.6
6	0	35.1	73.1	89.0	510.6	158.1	170.3	284.3	1021.1
7	5	37.0	73.1	93.2	617.8	164.9	182.3	302.6	1240.0
8	10	38.9	75.1	96.5	753.5	171.1	201.0	319.4	1601.7
9	15	40.7	81.1	98.8	847.8	175.8	214.7	345.4	1760.4
10	20	42.6	89.1	99.6	909.2	178.6	229.0	368.7	1864.1
11	25	44.5	93.8	99.3	984.5	181.1	251.3	397.4	2064.2

the oscillation of frequency due to any load demands and disturbances.

To demonstrate performance robustness of the proposed method, the ITAE and FD indices based on the system performance characteristics are being used as

$$\mathrm{ITAE} = 10 \times \int_0^{20} t(|\mathrm{ACE}_1(t)| + |\mathrm{ACE}_2(t)| + |\mathrm{ACE}_3(t)| + |\mathrm{ACE}_4(t)|)\mathrm{d}t$$
$$\mathrm{FD} = (\mathrm{OS} \times 30)^2 + (\mathrm{US} \times 10)^2 + Ts^2 \quad (27)$$

where overshoot (OS), undershoot (US) and settling time (for 5% band of the total load demand in area1) of frequency deviation area 1 is considered for evaluation of the FD. The values of ITAE and FD are calculated for the above scenarios whereas the system parameters are varied from −25% to 25% of the nominal values. The values of ITAE and FD for operation conditions under the scenarios 1 and 2 are listed in Tables 2 and 3 with and without SMES, respectively.

Examination of these Tables reveals that with the use of a small capacity SMES unit the system dynamic performances is significantly improved by the proposed robust mixed H_2/H_∞ controller designed in this paper against the plant parameters changes.

7. Conclusions

A new decentralized robust load frequency controller in the competitive electricity environment using the generalized LFC scheme model with considering SMES unit is proposed in this paper. Each control area contains different kinds of uncertainties and

Table 3
FD values with the mixed H_2/H_∞ and PI controllers

Test No	Parameter change (%)	Scenario 1				Scenario 2			
		With SMES		Without SMES		With SMES		Without SMES	
		Mixed	PI	Mixed	PI	Mixed	PI	Mixed	PI
1	−25	29.5	52.3	131.6	349.3	99.2	251.4	276.2	830.3
2	−20	29.2	58.0	127.6	345.6	100.0	280.7	279.1	902.5
3	−15	28.9	103.1	122.3	381.2	98.0	311.1	306.6	911.7
4	−10	28.6	111.2	118.4	535.0	96.1	357.8	360.7	984.4
5	−5	28.2	118.2	114.0	553.3	94.3	401.2	379.6	1089.3
6	0	27.9	124.3	110.5	625.7	91.5	420.3	342.8	1098.8
7	5	27.5	130.2	107.8	672.7	88.8	438.5	401.9	1127.9
8	10	28.2	136.2	105.9	714.6	86.1	456.7	443.5	1206.6
9	15	28.5	141.4	104.9	714.3	83.5	469.9	499.1	1371.4
10	20	28.8	145.7	135.8	702.1	81.2	476.7	513.6	1507.7
11	25	29.1	150.9	136.1	681.1	79.0	532.8	519.2	1519.3

disturbances because of increasing the complexity and change of power system structure. Thus, the LFC problem has been formulated as a decentralized multi-objective optimization control problem via a mixed H_2/H_∞ control approach and solved by LMI techniques to obtain optimal controller. Synthesis problem introduce appropriate uncertainties to consider of practical limits, has enough flexibility for setting the desired level of robust performance and leads to a set of relatively simple controllers, which are ideally practical for the real world complex power systems.

The effectiveness of the proposed strategy was tested on a four-area power system and compared with the PI controllers under possible contracts with various load changes in the presence of modeling uncertainties and GRC. The simulation results show that the proposed method is superior to the PI controllers and with the use of a small capacity SMES in some area the dynamic performance of system such as frequency regulation, tracking the load changes and disturbances attenuation is significantly improved for a wide range of plant parameter and area load changes. The system performance characteristics in terms of 'ITAE' and 'FD' indices reveal that the proposed robust controller with considering SMES unit is a promising control scheme for the solution of LFC problem and therefore it is recommended to generate good quality and reliable electric energy in the restructured power systems.

Appendix A. System data

Tables 4 and 5 shows power system parameters.

Table 4
GENCOs parameter

MVA_{base} (1000 MW) parameter	GENCOs (k in area i)							
	1-1	2-1	1-2	2-2	1-3	2-3	1-4	2-4
Rate (MW)	800	1000	1100	1200	1000	1000	900	1000
T_T (s)	0.36	0.42	0.44	0.40	0.36	0.40	0.38	0.40
T_H (s)	0.06	0.07	0.06	0.08	0.07	0.08	0.085	0.08
R (Hz/pu)	2.4	3.3	2.5	2.4	3	2.4	2	2.4
apf	0.5	0.5	0.6	0.4	0.5	0.5	0.5	0.5

Table 5
Control area parameters

Parameter	Area-1	Area-2	Area-3	Area-4
K_P (Hz/pu)	120	112.5	125	115
T_P (s)	20	25	20	25
B (pu/Hz)	0.425	0.385	0.359	0.425
K	0.63	1.15	0.89	0.29
T_{ij} (pu/Hz)	$T_{12} = 0.219$,	$T_{13} = 0.245$,	$T_{14} = 0.109$,	$T_{23} = 0.175$

Appendix B. SMES data

$L = 2.65$ H
$T_{dc} = 0.03$ s
$K_{SMES} = 100$ kV/unit MW
$K_{id} = 0.2$ kV/kA
$I_{d0} = 4.5$ kA

References

[1] Raineri R, Rios S, Schiele D. Technical and economic aspects of ancillary services markets in the electric power industry: an international comparison. Energy Policy 2006;34(13):1540–55.
[2] Feliachi A. On load frequency control in a deregulated environment. In: Proceedings of the IEEE international conference on control applications; 1996. p. 437–41
[3] Rerkpreedapong D, Hasanovic A, Feliachi A. Robust load frequency control using genetic algorithms and linear matrix inequalities. IEEE Trans Power Syst 2003;18(2):855–61.
[4] Liu F, Song YH, Ma J, Lu Q. Optimal load frequency control in restructured power systems. IEE Proc Gen Transm Dist 2003;150(1):87–95.
[5] Bevrani H, Mitani Y, Tsuji K. Robust decentralized AGC in a restructured power system. Energy Conver Manage 2004;45:2297–312.
[6] Donde V, Pai A, Hiskens IA. Simulation and optimization in a LFC system after deregulation. IEEE Trans Power Syst 2001;16(3):481–9.
[7] Scherer C, Gahinet P, Chilali M. Multi-objective output-feedback control via LMI optimization. IEEE Trans Automatic Control 1997;42(7):896–911.
[8] Scherer CW. Multi-objective mixed H_2/H_∞ control. IEEE Trans Automatic Control 1995;40(2):1054–62.
[9] Jaleeli N, Ewart DN, Fink LH. Understanding automatic generation control. IEEE Trans Power Syst 1992;7(3):1106–22.
[10] Elgerd OI. Electric energy system theory: an introduction. New York: McGraw-Hill; 1971.
[11] Banerjee S, Chatterjee JK, Tripathy SC. Application of magnetic energy storage unit as continuous var controller. IEEE Trans Energy Conver 1990;5(1):39–45.
[12] Tripathy SC, Kalantar M, Balasubramanian R. Dynamics and stability of wind and diesel turbine generators with superconducting magnetic energy storage unit on an isolated power system. IEEE Trans Energy Conver 1991;6(4):579–85.
[13] Banerjee S, Chatterjee JK, Tripathy SC. Application of magnetic energy storage unit as load frequency stabilizer. IEEE Trans Energy Conver 1990;5(1):46–51.
[14] Demiroren A, Yesil E. Automatic generation control with fuzzy logic controllers in the power system including SMES units. Elect Power Energy Syst 2004;26:291–305.
[15] Tripathy SC, Balasubramania R, Chanramohanan Nair PS. Effect of superconducting magnetic energy storage on automatic generation control considering governor deadband and boiler dynamics. IEEE Trans Power Syst 1992;3(7):1266–73.
[16] Abraham RJ, Das D, Patra A. Automatic generation control of an interconnected hydrothermal power system considering superconducting magnetic energy storage. Elect Power Energy Syst 2007;29:271–579.
[17] Shayeghi H, Shayanfar HA, Malik OP. Robust decentralized neural networks based LFC in a deregulated power system. Elect Power Syst Res 2007;47:241–51.
[18] Gahinet P, Nemirovski A, Laub AJ, Chilali M. LMI control toolbox. South Natick: The MathWorks Inc.; 2006.
[19] Djukanovic MB, Khammash MH, Vittal V. Sensitivity based structured singular value approach to stability robustness of power systems. IEEE Trans Power Syst 2000;15(2):825–30.

[20] Shayeghi H, Shayanfar HA. Robust decentralized LFC design in restructured power system. Int J Emerging Elect Power Syst 2006;7(1). 4/1–4/25.
[21] Skogested S, Postlethwaite I. Multivariable feedback control. John Wiley & Sons; 1996. pp. 449-467.
[22] Shayeghi H, Karrari M. Theory of μ synthesis for power systems load frequency control. J Elect Eng 2000;51:258–63.
[23] Shayeghi H, Shayanfar HA. Application of ANN technique based on μ-synthesis to load frequency control of interconnected power system. Elect Power Energy Syst 2006;28:503–11.

Hossein Shayeghi received the B.S. and M.S. degrees in Electrical and Control Engineering in 1996 and 1998, respectively. He received his Ph. D. degree in Electrical Engineering from Iran University of Science and Technology, Tehran, Iran in 2006. Currently, he is an Assistance Professor in Technical Eng. Department of University of Mohaghegh Ardebili, Ardebil, Iran. His research interests are in the Application of Robust Control, Artificial Intelligence to Power System Control Design, Operation and Planning and Power System Restructuring. He is a member of Iranian Association of Electrical and Electronic Engineers and IEEE.

Aref Jalili received the B.S. and M.S. degrees in Electrical Engineering from Azad University, Ardabil and South Tehran Branches, Iran in 2003 and 2005, respectively. Currently, he is a Ph. D. student in Electrical Engineering at Science and Technology Research Branch of the Azad University, Tehran, Iran. His areas of interest in research are Application of Fuzzy Logic and Genetic Algorithm to Power System Control and Restructuring.

Heidarali Shayanfar received the B.S. and M.S. degrees in Electrical Engineering in 1973 and 1979, respectively. He received his Ph. D. degree in Electrical Engineering from Michigan State University, U.S.A., in 1981. Currently, he is a Full Professor in Electrical Engineering Department of Iran University of Science and Technology, Tehran, Iran. His research interests are in the Application of Artificial Intelligence to Power System Control Design, Dynamic Load Modeling, Power System Observability Studies and Voltage Collapse. He is a member of Iranian Association of Electrical and Electronic Engineers and IEEE.